

Sebastian M. Torres  
Cooperative Institute for Mesoscale Meteorological Studies, University of Oklahoma  
Norman, Oklahoma

## 1. INTRODUCTION

It is well known that for Doppler radars transmitting uniformly spaced pulses there is a coupling between the unambiguous range ( $r_a$ ) and unambiguous velocity ( $v_a$ ) given by  $r_a v_a = c\lambda/8$ , where  $c$  is the speed of light and  $\lambda$  is the radar wavelength. As shown by this relation,  $r_a$  or  $v_a$  can only be increased at the expense of a proportional decrease in the other. This is a fundamental limitation since range and velocity ambiguity problems are coupled: trying to overcome one tends to worsen the other.

Over the last decade, the staggered PRT (pulse repetition time) technique has emerged as a viable candidate to address the mitigation of range and velocity ambiguities in the WSR-88D (Zrníc and Cook 2002). Its greatest potential is at intermediate elevations where ground clutter is not a major concern.

The staggered PRT technique has been thoroughly analyzed through theoretical and simulation studies but had not been implemented on the WSR-88D until recently. This paper describes a real-time implementation of the staggered PRT sampling and processing on NSSL's WSR-88D research radar.

## 2. AMBIGUITY MITIGATION IN THE WSR-88D

The possibility of range overlay and velocity aliasing in the WSR-88D has been well recognized, especially when observing severe phenomena involving large wind speeds. Accordingly, several mechanisms have been provided to alleviate ambiguity problems. Of interest here are those methods lying in the signal processing domain and which are currently implemented in the WSR-88D RDA (Radar Data Acquisition) unit.

At the lowest elevation angles, the WSR-88D performs two scans at each elevation angle. Each pair of cuts at the same elevation is usually referred to as a "split cut". The first scan uses a long PRT and produces power estimates (reflectivity) up to  $r_a = 460$  km. Velocity estimates from this scan are useless due to their low unambiguous velocity (about  $9 \text{ m s}^{-1}$ ). The second scan at the same elevation angle uses a short PRT ( $r_a = 148$  km) and produces (range folded) unambiguous velocities in the range up to  $v_a = 28 \text{ m s}^{-1}$ . Signal processing algorithms in the RDA use the long-PRT power data to unfold velocity estimates from the short-PRT scan to the proper range location. However, this

algorithm fails in regions where the overlaid powers in the short-PRT scan are within 10 dB of each other. Base data displays characterize this failure by encoding those range bins with overlaid powers using the color purple, normally referred to as the "purple haze".

At intermediate elevation angles, where clutter rejection requirements are less stringent, it is not necessary to run two uniform-PRT scans at the same elevation. In these cases, the WSR-88D reduces the time by running just one scan in the "batch mode" whereby long-PRT and short-PRT batches of pulses are interlaced. Analogously to the "split cut" processing, powers obtained from pulses at the long PRT ( $r_a > 233$  km) are used to unfold velocities from the short-PRT batch ( $v_a = 28 \text{ m s}^{-1}$ ). Unfortunately, as indicated before, not all overlaid powers can be recovered. As a result, during the observation of severe phenomena, it is typical to have significant areas of the velocity field obscured by the "purple haze".

At high elevation angles the occurrence of ambiguities is unlikely since storm tops do not exceed heights of about 21 km. Therefore, the system can safely operate at short PRTs providing larger aliasing intervals without the risk of range overlays.

## 3. THE STAGGERED PRT TECHNIQUE

The staggered PRT technique was first proposed in the context of weather surveillance radars by Sirmans et. al. (1976). With this technique, transmitter pulses are spaced at alternating PRTs  $T_1$  and  $T_2$ , (without loss of generality we assume  $T_1 < T_2$ ) and pulse-pair autocorrelation estimates are made independently for each PRT. These estimates are suitably combined so that the effective maximum unambiguous velocity becomes  $v_a = \lambda/[4(T_2 - T_1)]$  (Zrníc and Mahapatra, 1985). In addition, the unambiguous range is  $r_a = cT_1/2$ , corresponding to the shorter PRT. This implies that the staggered PRT is equivalent to a uniform PRT of  $T_2 - T_1$  for the unambiguous velocity and a uniform PRT of  $T_1$  for the unambiguous range, and each can be independently selected (Sachidananda and Zrníc, 2002).

The implementation of the staggered PRT technique on weather radars has been disqualified mainly due to the difficulties in designing efficient ground clutter filters. In addition, due to the non-uniform spacing between pulses, spectral processing of time series is a challenge. Moreover, since the pulse pair autocorrelation is obtained from independent pairs (as opposed to contiguous pairs as in the case of uniform PRT), slightly larger standard errors of estimates should be expected. Despite these disadvantages, the staggered PRT technique has emerged as a

---

*Corresponding author address:* Sebastian M. Torres, CIMMS/NSSL, 1313 Halley Circle, Norman, OK 73069; email: Sebastian.Torres@noaa.gov

complement to systematic phase coding in the quest to reduce the effects of velocity and range ambiguities on the WSR-88D.

#### 4. IMPLEMENTATION ON THE WSR-88D

A real-time implementation of the staggered PRT technique was completed on NSSL's KOUN research RDA (RRDA). NSSL's RRDA uses open-system standards and replaces most of the legacy WSR-88D RDA, especially the functions associated with the signal processor (Zahrai et al. 2002). The bulk of the signal processing is performed by an array of PowerPC 7400 processors linked by a high-speed interconnect. The resulting system replicates the functionality of the legacy RDA, and its expandability characteristics make it the perfect platform to implement new algorithms.

The RRDA synchronizer generates timing signals for any PRT between 760 and 2200  $\mu$ s with a resolution given by the 9.6 MHz system clock. In addition, it is possible to change the PRT on a pulse-by-pulse basis. This is particularly advantageous for generating staggered PRT sequences with precise  $T_1/T_2$  ratios.

The staggered PRT algorithm was tailored to allow a seamless insertion into the current signal processing pipeline (Torres and Zahrai 2002). The implementation incorporates new functionality (e.g., clutter filtering, velocity dealiasing, data censoring) but matches the legacy WSR-88D functionality when appropriate (e.g., interference suppression, strong point clutter censoring). Staggered PRT radials are characterized by a transmission sequence that alternates two PRTs,  $T_1$  and  $T_2$  for a total of  $M$  pulses. As mentioned above, assume that  $T_1$  is the short PRT and  $T_2$  is the long PRT. In this first implementation, we also assume that there are no storms beyond  $r_{a2} = cT_2/2$ . That is, echoes from the short PRT can overlay part of the ones from the long PRT, but not vice versa. A technique to resolve more complex overlay situations is given by Sachidananda and Zrnich (2003).

Incoming in-phase ( $I$ ) and quadrature phase ( $Q$ ) data are corrected for AGC (automatic gain control) imperfections and phase detector imbalances. In addition, data showing interference are removed to avoid moment estimate biases. Powers ( $P_1, P_2$ ) and pulse-pair autocorrelations ( $R_1, R_2$ ) are computed for  $T_1$  and  $T_2$ , and a simple map-based clutter filter is applied to them. While  $P_2$  is computed up to  $r_{a2}$ ,  $P_1, R_1$ , and  $R_2$  can only be computed up to  $r_{a1}$ . The clutter filtering algorithm removes the magnitude squared of the  $I$  and  $Q$  mean (or DC) component in those locations where the site-dependent clutter filter bypass map indicates the need for clutter filtering. In addition, strong point clutter is removed from powers and correlation vectors.

Doppler velocities  $v_1$  and  $v_2$  are computed from  $R_1$  and  $R_2$ , the pulse-pair autocorrelation estimates corresponding to  $T_1$  and  $T_2$ . As suggested by Sachidananda and Zrnich (2002), the difference of the two velocity estimates is used to determine the aliasing interval of the true velocity, and the velocity estimate corresponding to the shorter PRT is dealiased using this information. Table 1 shows the rules used in the

dealiasing algorithm. Note that the number of rules to evaluate increases as the staggered PRT ratio approaches 1 (the current version of the algorithm deals with PRT ratios of up to 4/5).

If $T_1/T_2$	... and $v_1 - v_2$ is closest to	... adjust $v_1$ by adding
= 1/2, 2/3, 3/4, or 4/5	0	0
	$2v_{a2}$	0
	$-2v_{a2}$	0
= 2/3, 3/4, or 4/5	$-2v_{a1} + 2v_{a2}$	$2v_{a1}$
	$2v_{a1} - 2v_{a2}$	$-2v_{a1}$
= 3/4 or 4/5	$-2v_{a1} + 4v_{a2}$	$2v_{a1}$
	$2v_{a1} - 4v_{a2}$	$-2v_{a1}$
= 4/5	$-4v_{a1} + 4v_{a2}$	$4v_{a1}$
	$4v_{a1} - 4v_{a2}$	$-4v_{a1}$

**Table 1.** Rules for the velocity dealiasing algorithm.  $v_{a1} = \lambda/4T_1$  and  $v_{a2} = \lambda/4T_2$  are the maximum unambiguous velocities for  $v_1$  and  $v_2$ , respectively.

The spectrum width is computed as in the legacy WSR-88D but only using the powers and pulse-pair autocorrelations corresponding to the longer PRT ( $T_2$ ), which yield lower errors of estimates (Zrnich and Mahapatra, 1985).

To compute the reflectivity, data are extracted from the two power arrays  $P_1$  and  $P_2$  with different rules for each of the three segments depicted in Figure 1. For segment I, data are extracted only from  $P_1$ , since  $P_2$  may be contaminated on those range bins with overlaid powers. An average of  $P_1$  and  $P_2$  is extracted for segment II, given that both power vectors are "clean" there. Finally, segment III data are obtained from  $P_2$ .

Censoring of velocity and spectrum width data is only necessary in segment I. This is done by analyzing  $P_1$  in segment I and  $P_2$  in segment III. The idea is to determine whether second trip signals mask first trip signals in segment I of  $P_2$ . While such overlaid echoes appear in every other pulse and do not bias velocity estimates at those range locations, overlaid powers act as noise. Therefore, when second trip powers in segment I of  $P_2$  are above a preset fraction of their first trip counterparts, the corresponding velocity and spectrum width estimates exhibit very large errors and must be censored.

As a final step, all moments are thresholded based on the SNR (signal-to-noise ratio), and data are scaled and formatted to be received, displayed, and processed by the RPG (Radar Product Generation) unit.

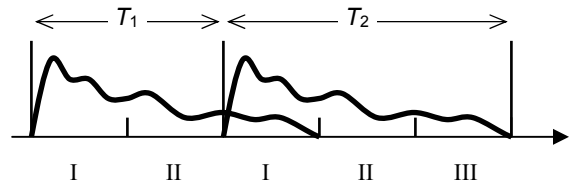


**Figure 1.** Signal powers in the staggered PRT algorithm. Roman numerals indicate segment numbers used in the reflectivity computation and censoring algorithms.

## 5. EXPERIMENTAL RESULTS

Staggered PRT data was collected and processed in real time using NSSL's KOUN radar in Norman, OK. The case in Fig. 2 was obtained on February 13, 2003 at 20:57 GMT. KOUN ran a scan at 0.5 deg using the staggered PRT mode where  $T_1 = 3.107$  ms ( $r_{a1} = 466$  km) and  $T_2 = 2.24$  ms ( $r_{a2} = 336$  km) with  $M = 64$  pulses. Note that  $T_1/T_2 = 0.72$  and the resulting composite maximum unambiguous velocity is  $v_a = 32$  m s<sup>-1</sup>.

Fig. 3 shows Doppler velocity display for the same event as observed by the KTLX radar in Twin Lakes, OK (located about 20 km to the north of KOUN). The time is 20:58 GMT and the elevation angle is 0.5 deg. This corresponds to the second half of a "split cut" in the WSR-88D. KTLX ran a scan with a uniform long PRT of 3.107 ms followed by a scan with a uniform short PRT of 0.987 ms. The maximum unambiguous velocity is  $v_a = 26.1$  m s<sup>-1</sup>.

As expected, KTLX's Doppler velocity display is significantly obscured by the "purple haze" (here in white for viewability) which indicates the presence of unresolvable overlaid echoes. An additional limitation is that KTLX, like all NEXRAD radars, only displays velocities up to 230 km. KOUN displays velocities without obscuration up to a maximum range of  $cT_1/2$  or 336 km in this case (only up to about 200 km are shown in Figs. 2 and 3). While velocity estimates agree fairly well in places where both radars show valid data, estimates obtained with the staggered PRT algorithm can alias in places of low SNR. On top of this, the performance of the simple ground clutter filter implemented in this version of the staggered PRT algorithm is inferior compared to the recursive ground clutter filter used in the WSR-88D with uniform PRT sequences. Evidence of this is the velocity bias towards zero observed on range bins close to the radar when comparing KOUN with KTLX velocities.

## 6. CONCLUSIONS

This paper described a real-time implementation of staggered PRT sampling and processing on NSSL's WSR-88D research radar. The algorithm was tailored to allow a seamless insertion into the legacy signal processing pipeline and includes a simple map-based ground clutter filter. Operational tests show that the computational complexity of this method is well within the expected capabilities of the next generation ORDA (open radar data acquisition). Preliminary results included in this work demonstrate that the staggered PRT technique is a feasible candidate for mitigating range and velocity ambiguities in future enhancements of the national network of weather surveillance radars.

## 7. REFERENCES

Sachidananda, M. and D. Zrnica, 2002: An improved clutter filtering and spectral moment estimation algorithm for staggered PRT sequences. *J. Atmos. Oceanic Technol.*, **19**, 2009-2019.

- Sachidananda, M. and D. Zrnica, 2003: Unambiguous range extension by overlay resolution in staggered PRT technique. *J. Atmos. Oceanic Technol.*, **20**, 673-684.
- Sirmans, D., D. Zrnica, and B. Bumgarner, 1976: Extension of maximum unambiguous Doppler velocity by use of two sampling rates. *Preprints 17<sup>th</sup> Conf. on Radar Meteorology*, Seattle, WA, Amer. Meteor. Soc., pp. 23-28.
- Torres, S. and A. Zahrai, 2002: Migration of WSR-88D signal processing functionality to open systems. *Preprints 18<sup>th</sup> International Conf. on IIPS*, Orlando, FL, Amer. Meteor. Soc., paper 5.11.
- Zahrai, A., S. Torres, I. Ivic, and C. Curtis, 2002: The open radar data acquisition (ORDA) design for the WSR-88D. *Preprints 18<sup>th</sup> International Conf. on IIPS*, Orlando, FL, Amer. Meteor. Soc., paper 5.10.
- Zrnica, D. and R. Cook, 2002: Evaluation of techniques to mitigate range and velocity ambiguities on the WSR-88D. *Preprints 18<sup>th</sup> International Conf. on IIPS*, Orlando, FL, Amer. Meteor. Soc., paper 5.13.
- Zrnica, D., and P. Mahapatra, 1985: Two methods of ambiguity resolution in pulse Doppler weather radars. *IEEE Trans. Aerosp. Electron. Syst.*, **21**, 470-483.

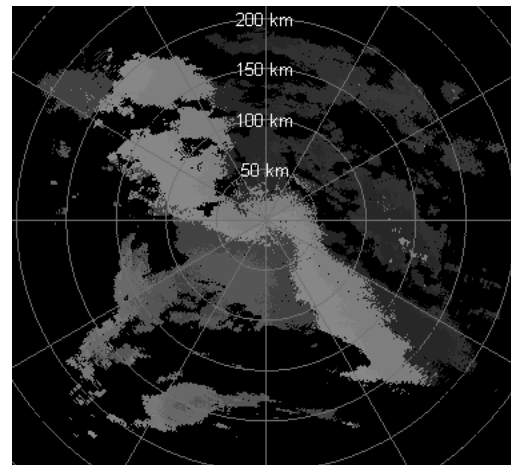


Figure 2. KOUN's Doppler velocity display.

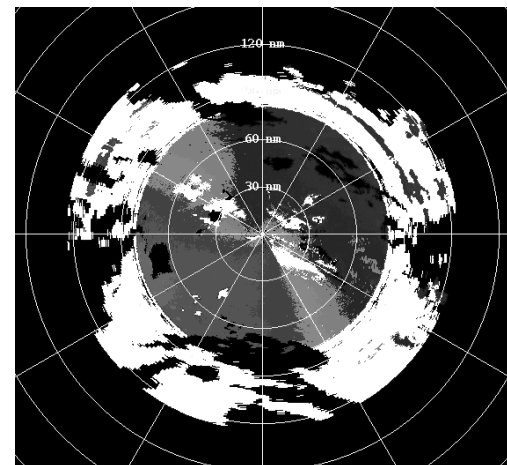


Figure 3. KTLX's Doppler velocity display.